Selected Paper

Photochemical Behavior of an Anthracene–Urea Derivative Interacting with Anions

Ikuma Ohshiro, Masashi Ikegami, Yoshihiro Shinohara, Yoshinobu Nishimura, and Tatsuo Arai*

Graduate School of Pure and Applied Sciences, University of Tsukuba, Tsukuba 305-8571

Received August 25, 2006; E-mail: arai@chem.tsukuba.ac.jp

The synthesis and photophysical properties of a fluorescent anthracene–urea derivative, which can associate with anions, such as acetate or phosphate, by hydrogen-bonding, are reported. A new anthracene derivative bearing phenylurea group at the 9-position of anthracene, 1-anthracen-9-yl-3-phenylurea, (9PUA) was prepared. 9PUA was found to exhibit strong selectivity in relation to anions, some of which showed a remarkable change in emission. 9PUA had a monomer emission maximum at 450 nm, and the monomer emission was quenched to give a new emission with a maximum at 580 nm on the addition of acetate anion. The emission at 580 nm was assigned to a tautomer form of 9PUA generated by intermolecular proton transfer as a result of an excited-state reaction with acetate anion.

The development of luminescent chemosensors for the detection of cations, anions, and neutral molecules is very interesting in the practical point of view, so that many studies have been reported.[1–4] With the aid of supramolecular chemistry that uses hydrogen-bonding ability, recognizing and sensing of anionic analytes have recently emerged as a key research field. Several applications, such as a luminescent molecular logic gate[5,6] and colorimetric sensing ensemble,[7–9] should be possible.

Urea derivatives are frequently utilized as sensors for several anions, while some aromatic compounds, such as naphthalene, anthracene, and pyrene, are generally known as chromophores. When certain anions associate with the sensing part of a chemosensor, some spectroscopic changes have often been observed. For example, new absorption bands have appeared as a result of the interaction with an anion,[10–13] remarkable changes in fluorescence intensity have been observed in the presence of an anion,[14–19] and new emission bands have emerged in lower energy regions due to complex formation.[20–22] Especially, fluorescence spectroscopy has been one of the most important detection methods due to its simplicity and high detection efficiency, and NMR titrations are also a promising method for quantitatively detecting anions.[23–26]

In this research, we synthesized the compound 9PUA having a simple structure with host and emission moieties in the molecule. The structure of 9PUA is shown in Fig. 1, and the anthracene ring and urea moiety function as fluorescent and recognition parts, respectively. Fluorescence analysis was used to detect the changes in hydrogen-bonding interaction between 9PUA and a target molecule with sufficient accuracy. Biologically relevant anions, such as phosphate, acetate, and bromide, were chosen as guest anions. The resulting species associated with 9PUA in DMSO showed a characteristic emission band around 580 nm along with normal emission maximized at 450 nm, which is ascribed to the locally excited state of 9PUA (9PUA*). This indicates that a new electronic state formed in the presence of the anion in the excited state (**X***). Thus, anion recognition takes place through hydrogen-bonding between the urea hydrogens and the anion, followed by formation of a complex. Steady and time-resolved emission spectroscopy were performed to investigate **X*** located at longer wavelength. It was confirmed that the addition of anion to 9PUA promoted the formation of **X*** which followed a decrease in emission intensity from 9PUA*. Since no differences in the location and width of **X*** emission between acetate and phosphate were observed, it is plausible to assign **X** as a tautomer of 9PUA formed by the interaction with an anion.

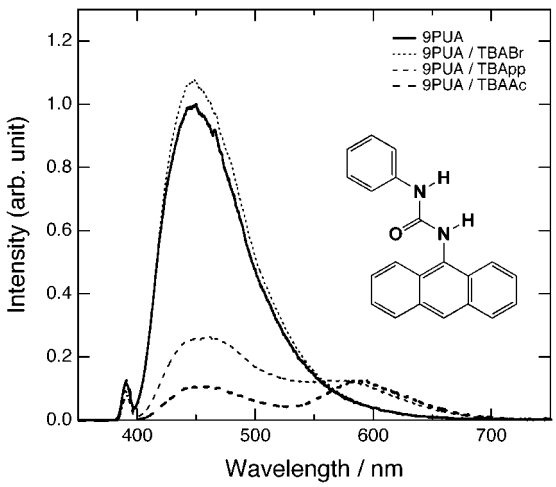

Fig. 1. Fluorescence spectra of 9PUA (1.0×10^{-5} M) and 9PUA in the presence of 10 mM TBA salts (TBABr, TBApp, and TBAAc) in DMSO.

Results and Discussion

Absorption and Fluorescence Spectra. Figure 1 shows fluorescence spectra of 9PUA (1.0×10^{-5} M, 1 M = 1 mol dm^{-3}) in DMSO in the absence and presence of various tetrabutylammonium (TBA) salts: acetate (TBAAc), phosphate (TBApp), and bromide (TBABr). Remarkable changes in

Published on the web April 13, 2007; doi:10.1246/bcsj.80.747

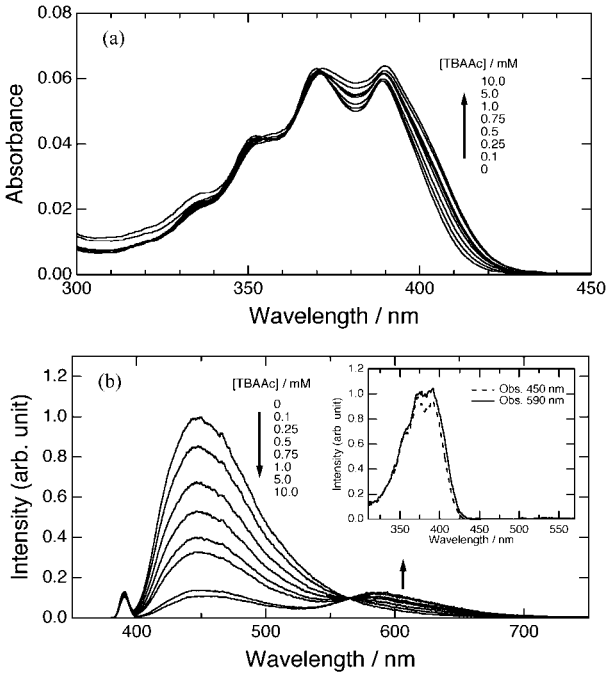

Fig. 2. Change in the (a) absorption and (b) fluorescence spectra of 9PUA (1.0×10^{-5} M) upon addition of TBAAc (0–10 mM) in DMSO. The inset of (b) represents excitation spectra observed at 450 nm (broken line) and 590 nm (solid line) in the presence of 10 mM TBAAc in DMSO normalized at 372 nm.

emission spectra were observed in the presence of TBAAc and TBApp, although no significant changes in the spectral shape of emission spectrum corresponding to 9PUA*, except for a slight increase in the intensity, were observed in the presence of TBABr. This result implies that the fluorescence quenching of 9PUA* is not directly caused by a dynamic interaction between the excited 9-anthrylurea group and the anion accompanied by a diffusion process, but by a hydrogen-bonding interaction between the urea group and the anion in the ground state. Furthermore, these phenomena indicated that the interaction between 9PUA and the anions depends on the properties of anions in its coordination manner with 9PUA. In the case of TBAAc and TBApp, the intensity of 9PUA* emission obviously decreased, and a new fluorescence band appeared around 580 nm corresponding to **X*** in contrast to those of TBABr. The specific interaction between 9PUA and anion must be responsible for the formation such a longer stable emissive species.

The concentration dependence of the absorption and emission spectra from 9PUA* and **X*** in the case of TBAAc were investigated, since the spectra from 9PUA* and **X*** had no significant differences between TBAAc and TBApp. The absorption spectra of 9PUA upon the addition of TBAAc in DMSO are shown in Fig. 2a. The absorption maxima of 9PUA appeared at wavelengths similar to those of anthracene (351, 370, and 389 nm). Spectral red shift of the absorption band above 400 nm and broadening especially around 380 nm were observed on the addition of TBAAc. The fluorescence spectra of 9PUA in DMSO are shown in Fig. 2b. Remarkable changes in the fluorescence spectra of 9PUA, which is responsible for

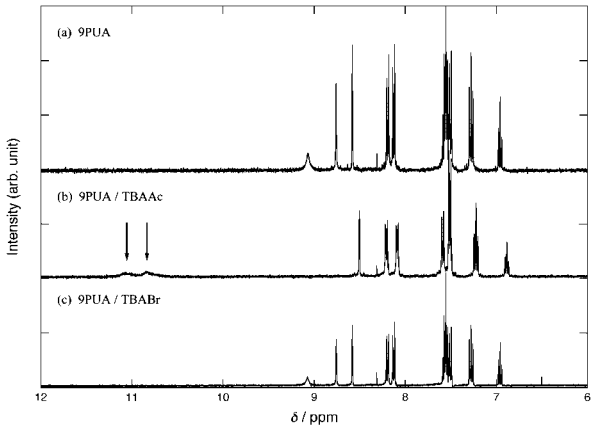

Fig. 3. ^{1}H NMR spectra of (a) 9PUA (5.0×10^{-3} M), (b) 9PUA in the presence of TBAAc (9PUA/TBAAc), and (c) 9PUA in the presence of TBABr (9PUA/TBABr) in DMSO-d_6. The concentration of TBA salts was 5.0×10^{-3} M.

an anthracene ring, were observed, while the red shift was estimated to be a small change within 2 nm. In Fig. 2b, the fluorescence intensity of 9PUA observed at 450 nm was monotonically quenched with an increase in the concentration of TBAAc, while a new long-wavelength emission maximized at 580 nm. An isosbestic point simultaneously appeared at 565 nm in the presence of TBAAc above 5 mM. These results imply that the addition of anion to 9PUA induces the formation of **X*** as a result of quenching of 9PUA* by TBAAc. It is worthwhile to note that Stokes shift corresponding to **X*** was a relatively large ($8300\,cm^{-1}$) in comparison to that of normal emission ($3480\,cm^{-1}$). The inset of Fig. 2b shows the excitation spectra monitored at 450 and 590 nm upon the addition of 10 mM of TBAAc, which mainly correspond to the emission from 9PUA* and **X***, respectively. The spectra observed at 450 and 590 nm are very similar to those in the absence and presence of TBAAc in comparison with Fig. 2a. In addition, there was no significant spectrum longer than 450 nm when monitor wavelength was 590 nm. This indicated that the **X*** emission originates from the excitation of red-shifted component as shown in Fig. 2a.

^{1}H NMR Experiment. ^{1}H NMR spectroscopy has been widely used to investigate receptor–substrate interactions, and it allows us to study the details of the interaction between compound 9PUA and TBAAc. Therefore, ^{1}H NMR spectra of 9PUA with or without TBAAc in DMSO-d_6 at 20 °C were measured to elucidate how 9PUA and TBAAc bind together. Figure 3 shows ^{1}H NMR spectra of 9PUA in the absence and presence of TBA salts in DMSO-d_6. The concentration of 9PUA and each TBA salt was 5.0×10^{-3} M. The NMR spectrum of 9PUA had two characteristic peaks: one small and broadened signal at 9.08 ppm due to the NH proton of one urea group and another signal at 8.77 ppm due to the NH proton that is adjacent to the anthracene ring. Both signals of the NH protons in the presence of TBAAc shifted markedly downfield to 11.07 and 10.85 ppm, although the other anthracene H signals remained almost unchanged as shown in Fig 3b. A similar observation was made in the case of TBApp (data not shown). The spectrum of 9PUA/TBABr was found

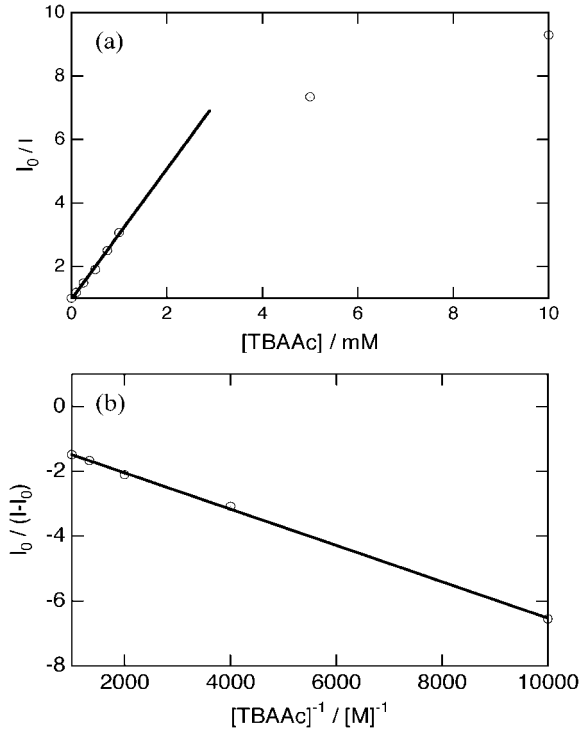

Fig. 4. (a) Stern–Volmer plot of 9PUA quenched by TBAAc (see text in details). (b) Theoretical fit (solid line) of Eq. 2 to $I_0/(I - I_0)$ against $[\mathrm{TBAAc}]^{-1}$.

to be totally the same as that of 9PUA. Considering these results, 9PUA and acetate generate a complex via hydrogen-bonding interactions between the urea and carboxyl groups in 9PUA/TBAAc.

Stern–Volmer Analysis. Figure 4a represents the Stern–Volmer plot of 9PUA quenched by TBAAc, where I_0 and I stand for the fluorescence intensity at 450 nm in the absence and presence of TBAAc, respectively and they were corrected by the absorbance at 450 nm due to the spectral change in the presence of TBAAc. A linear relationship between I_0/I and [TBAAc] up to 1 mM was obtained, and then the plot deviated from a straight line corresponding to a slow increase in I_0/I, indicating a strong interaction between 9PUA and TBAAc in the ground and excited states above 1 mM of TBAAc. A plot of I_0/I vs [TBAAc] up to 1 mM gave a Stern–Volmer constant ($k_q\tau_s$) of 2050 M^{-1}, and therefore, the rate constant of fluorescence quenching (k_q) was determined to be $8.4 \times 10^{11}\ \mathrm{M}^{-1}\ \mathrm{s}^{-1}$ by using $\tau_s = 2.44$ ns as listed in Table 1. It is noted that diffusion-controlled rate of DMSO solution has been reported to be $3.0 \times 10^9\ \mathrm{M}^{-1}\ \mathrm{s}^{-1}$.[27] The value of k_q seems to be larger than the diffusion-controlled rate constant, indicating that TBAAc exists in close contact to 9PUA even when the concentration of TBAAc is less than 1 mM. Furthermore, the association constant (K_a) of this complex was determined from the variation of fluorescence intensity at the appropriate observation wavelengths. For the complex of 1:1 stoichiometry, K_a can be written as $K_a = [\mathrm{HA}]/[\mathrm{H}][\mathrm{A}]$, where [HA], [H], and [A] are corresponding to the concentrations of complex, HA, host, H, and anion, A, respectively. The following equations can be derived from the relation between fluorescence intensity and the concentration of host or complex:[28]

Table 1. Fluorescence Lifetimes of 9PUA Observed at 450, 510, and 590 nm in the Absence and Presence of Various Anions[a)]

	τ/ns		
Anion	450 nm	510 nm	590 nm
none	2.44 (1.000)	2.46 (1.000)	2.45 (0.979) 11.63 (0.021)
TBAAc[b)]	2.15 (1.000)	2.15 (1.000)	2.21 (0.933) 11.94 (0.067)
TBAAc[c)]	0.15 (0.758) 2.39 (0.242)	0.16 (0.816) 2.47 (0.184)	0.14 (0.670) 2.21 (0.103) 11.21 (0.227)
TBApp[c)]	0.49 (0.770) 2.31 (0.230)	0.60 (0.803) 2.38 (0.197)	1.24 (0.791) 11.02 (0.209)
TBABr[c)]	1.17 (0.103) 2.64 (0.897)	2.34 (0.705) 2.98 (0.295)	2.54 (0.980) 8.61 (0.020)

a) Normalized amplitudes are shown in the parenthesis in the case of multiexponential decay. b) 0.25 mM. c) 10 mM.

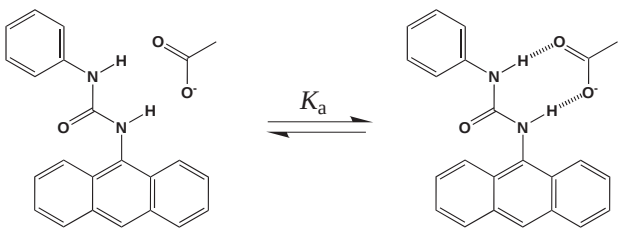

Scheme 1. Plausible hydrogen bonding between 9PUA and TBAAc.

$$\frac{I - I_0}{I_{\max} - I} = K_a[\mathrm{A}], \tag{1}$$

$$\frac{I_0}{I - I_0} = \frac{I_0}{I_{\max} - I_0}\left(\frac{1}{K_a[\mathrm{A}]} + 1\right), \tag{2}$$

where I_0 and I are the fluorescence intensity of host monitored at 450 nm in the absence and presence of anion, respectively, and [A] is the total concentration of anion. $I_{\max}$ is the fluorescence intensity of fully hydrogen-bonded 9PUA with anion. Equation 2 is a derivation of Eq. 1 to determine K_a without knowing $I_{\max}$, because the first term of right side of Eq. 2 must be constant. A plot of $I_0/(I - I_0)$ against $[\mathrm{TBAAc}]^{-1}$ gave a good linear relationship as shown in Fig. 4b, if [A] < 0.001 M, and showed that 9PUA forms a 1:1 stoichiometric complex with TBAAc with $K_a = 1600\ \mathrm{M}^{-1}$. Taking into account the results from NMR and fluorescence quenching, a probable structure for the complex is shown in Scheme 1, and it is thought to be responsible for the red-shifted component in Fig. 2a.

Fluorescence Decay. Table 1 lists the fluorescence lifetimes of 9PUA in the absence and presence of various anions under Ar. All decays were analyzed by using a multiexponential function to give lifetimes and normalized amplitudes. In the absence of anions, decays observed at 450 and 510 nm were calculated to be 2.44 and 2.46 ns, respectively, with a single-exponential function and decay at 590 nm consists of two components with 2.45 and 11.63 ns. Contribution of the longer lifetime is negligibly small. In the presence of 0.25 mM of

TBAAc, small amount of fluorescence quenching was observed to be 2.15, 2.15, and 2.21 ns at 450, 510, and 590 nm, respectively, which is consistent with the steady-state quenching results shown in Fig. 2b. At this concentration, the excited state of uncomplexed 9PUA seemed to be dynamically quenched by TBAAc. The fluorescence decay curves obtained at 10 mM of TBAAc had two components and were estimated to be 0.15 and 2.39 ns, 0.16 and 2.47 ns monitored at 450 and 510 nm, respectively. The contribution of 11 ns component became larger than that at 0.25 mM TBAAc, while the lifetime components at 590 nm were 0.14, 2.21, and 11.21 ns. From the fluorescence-quenching measurement, shown in Fig. 2b, the intensity of the peak for $\mathbf{X}^*$ increased with the concentration of TBAAc accompanied by a decrease in that for 9PUA*. From these results, $\mathbf{X}^*$ was determined to be the emissive species that has ca. 11 ns lifetime. Although the 10 mM TBAAc may be responsible for fluorescence quenching leading to the component of 0.15 ns, the component of 2.39 ns, comparable to that of 9PUA* in the absence of anions, seems to reflect some circumstances surrounding 9PUA like avoidance of dynamic quenching by TBAAc. This phenomenon is also confirmed in the case of TBApp, which is a less efficient quencher than TBAAc because of prolonged lifetime of 0.60 ns compared to 0.16 ns in TBAAc monitored at 510 nm. Interestingly, the components observed at 590 nm, which is ascribed to $\mathbf{X}^*$, had no rise-up lifetimes. This means that the formation of $\mathbf{X}^*$ originates not from dynamic quenching of 9PUA by anion, but from static quenching of complex between 9PUA and anion that already exists in the ground state. The time constant corresponding to the formation of $\mathbf{X}^*$ may be within 1 ps considering time resolution of the present system. In the case of TBABr, it is notable that the lifetimes observed at all wavelengths were slightly longer than those in the absence of anion. This is consistent with the steady-state measurement as shown in Fig. 2b, reflecting enhanced emission in the presence of TBABr.

Time-Resolved Fluorescence Spectra. Figure 5 shows time-resolved spectra of 9PUA in the presence of 10 mM of TBAAc excited at 375 nm under Ar. Each fluorescence spectrum was made from time slices of fluorescence decays measured from 390 to 670 nm with a 2 nm wavelength interval, and normalized at the corresponding maximum intensity without correcting for the sensitivity of the detector. Time zero was determined by the peak position of instrument response function monitored at 375 nm. The spectra just after excitation exhibited an emission maximum at 450 nm, which originates from 9PUA*, along with long tail up to 650 nm. The emission spectrum maximized at 580 nm, which is ascribed to $\mathbf{X}^*$, appeared at 0.48 ns instead of 0 ns. The relative intensity of $\mathbf{X}^*$ to 9PUA* increased with time, and $\mathbf{X}^*$ became predominant at 18.96 ns. Note that no rise component of $\mathbf{X}^*$ was derived from lifetime analysis, indicating that time development of 9PUA* and $\mathbf{X}^*$ reflects differences in corresponding lifetime between them. Since no spectral shifts of 9PUA* and $\mathbf{X}^*$ were observed within measured time region, it implies that emissive states of 9PUA* and $\mathbf{X}^*$ remain unchanged and no other species exist including structurally relaxed conformers.

Relaxation Mechanism of 9PUA*. Present results suggest that the complex formed between 9PUA and an anion in the ground state is involved in the emission from $\mathbf{X}^*$. This is supported by the fact that excitation spectrum monitored at 590 nm was similar to the absorption spectrum at the same concentration of TBAAc. On the other hand, $\mathbf{X}^*$ had a relatively large Stokes shift of 8300 cm^{-1} in comparison with 3480 cm^{-1} in normal emission. Conformational changes are necessary to explain this phenomenon. In addition, time-resolved measurements indicated that the formation of $\mathbf{X}^*$ took place less than a picosecond, since the emission of **X** has no rise components in the decay observed at 590 nm. Photoirradiation afforded the excited state of complex followed by formation of emissive tautomer via proton transfer as shown in Scheme 2. It is well known that hydrogen atom transfer in the excited state occurs in less than ps time region and that a tautomer has a large Stokes shift in general.[29]

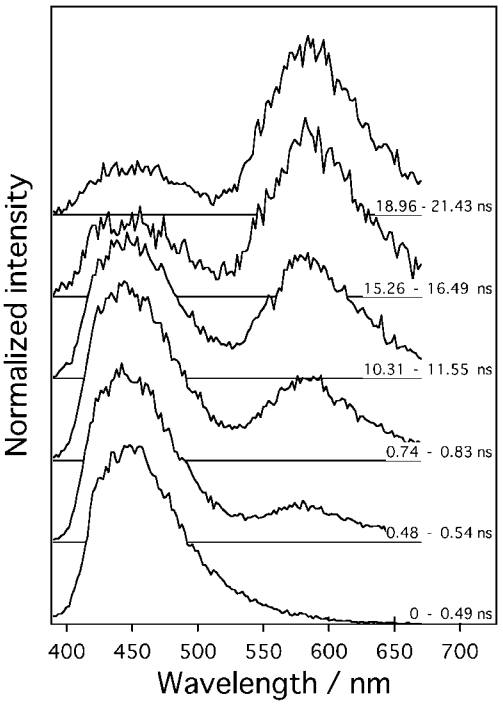

Fig. 5. Time-resolved fluorescence spectra of 9PUA (1.0×10^{-5} M) in the presence of TBAAc (10 mM) excited at 375 nm under Ar.

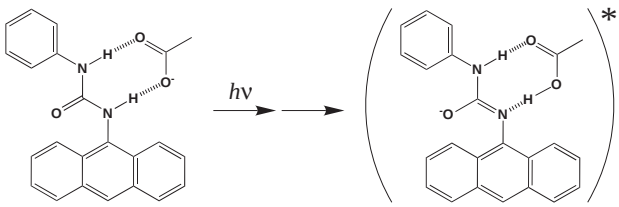

Scheme 2. Reaction scheme for $\mathbf{X}^*$ formation upon irradiation of the complex.

Conclusion

Consequently, we showed that 9PUA interacts with TBAAc in the ground state by hydrogen-bonding interaction affording a 1:1 complex of 9PUA and TBAAc, determined from quantitative analysis of fluorescence-quenching measurement.

^{1}H NMR experiment spectroscopy showed that the urea and carboxyl groups are involved in complex formation. Furthermore, the fluorescence quenching and the appearance of a new emission band verified the formation of a tautomer from a complex between 9PUA and an anion.

Time-resolved measurement should be a useful methodology to elucidate reaction kinetics in the excited state in conjunction with other steady-state method.

Experimental

Methods. Absorption and fluorescence spectra were measured on a Shimadzu UV-1600 and on a Hitachi F-4500 fluorescence spectrometer, respectively. Fluorescence decay measurements were performed by using a time-correlated single-photon counting method.[30] Laser excitation at 375 nm was achieved by using a diode laser (PicoQuant, LDH-P-C-375) with a power control unit (PicoQuant, PDL 800-B) in a repetition rate of 2.5 MHz. Temporal profiles of fluorescence decay were detected by using a microchannel plate photomultiplier (Hamamatsu, R3809U) equipped with a TCSPC computer board module (Becker and Hickl, SPC630). Full-width at half-maximum (FWHM) of the instrument response function was 51 ps. The values of χ^2 and the Durbin–Watson parameters were used to determine the quality of the fit obtained by nonlinear regression.[31] DMSO (for spectroscopy, Wako Chem. Japan) was used as a solvent without further purification. All measurement were carried out at room temperature under Ar. The concentration was adjusted so that the absorption maximum of the excitation wavelength was 0.1 for each sample. ^{1}H NMR spectra were measured on a 400 MHz NMR spectrometer, ARX-400.

Synthesis. 1-Anthracen-9-yl-3-phenylurea (9PUA): Triethylamine (100 μL, ca. 0.74 mmol) was added to a suspension of anthracene-9-carboxylic acid (150 mg, 0.68 mmol) in toluene, and the mixture was stirred at 40 °C under nitrogen for 30 min. Then, diphenylphosphoryl azide (60 μL, 0.74 mmol) was added to the reaction mixture, and the resulting solution was stirred at 80 °C under nitrogen for 30 min. Aniline (68.9 mg, 0.74 mmol) was dissolved in toluene (5 mL) and the toluene solution was added to the reaction mixture. After the reaction mixture was stirred at 80 °C for 4 h, it was cooled to room temperature and then, the solvent was remove by evaporation. The residue was extracted with dichloromethane and washed with water. After the solvent was removed, the residue was purified by recrystallization from chloroform to give a light yellow powder (50 mg, 0.16 mmol; yield 24%): mp > 210 °C. Anal. Calcd for $C_{21}H_{16}N_2O$: C, 80.75; H, 5.16; N, 8.97%. Found: C, 80.72; H, 5.17; N, 8.63%. ^{1}H NMR ($CDCl_3$, 400 MHz): δ 9.08 (brs, 1H, –NH), 8.77 (s, 1H, –NH), 8.58 (s, 1H, anthryl), 8.19 (d, 2H, $J = 9.2$ Hz, anthryl), 8.13 (d, 2H, $J = 9.2$ Hz, anthryl), 7.60–7.53 (m, 4H, anthryl), 7.53–7.48 (m, 2H, phenyl), 7.28 (t, 2H, $J = 8.0$ Hz, phenyl), 6.96 (t, 1H, $J = 7.2$ Hz, phenyl).

This work was supported by a Grant-in-Aid for Scientific Research on Priority Areas (417), a Grant-in-Aid for Scientific Research (Nos. 16350005 and 16550115) and the 21st Century COE Program from the Ministry of Education, Culture, Sports, Science and Technology (MEXT) of the Japanese Government, by University of Tsukuba Research Projects.

References

1 P. A. Gale, *Coord. Chem. Rev.* **2000**, *199*, 181.
2 R. Martínez-Máñez, F. Sancenón, *Chem. Rev.* **2003**, *103*, 4419.
3 C. Suksai, T. Tuntulani, *Chem. Soc. Rev.* **2003**, *32*, 192.
4 T. W. Bell, N. M. Hext, *Chem. Soc. Rev.* **2004**, *33*, 589.
5 T. Gunnlaugsson, D. A. M. Dónaila, D. Parker, *Chem. Commun.* **2000**, 93.
6 A. P. de Silva, B. McCaughan, B. O. F. McKinney, M. Querol, *J. Chem. Soc., Dalton Trans.* **2003**, 1902.
7 J. J. Lavigne, E. V. Anslyn, *Angew. Chem., Int. Ed.* **1999**, *38*, 3666.
8 Z. Zhong, E. V. Anslyn, *J. Am. Chem. Soc.* **2002**, *124*, 9014.
9 S. C. McCleskey, A. Metzger, C. S. Simmons, E. V. Anslyn, *Tetrahedron* **2002**, *58*, 621.
10 S. Nishizawa, P. Biihlmann, M. Iwao, Y. Umezawa, *Tetrahedron Lett.* **1995**, *36*, 6483.
11 R. Kato, S. Nishizawa, T. Hayashita, N. Teramae, *Tetrahedron Lett.* **2001**, *42*, 5053.
12 M. Boiocchi, L. D. Boca, D. E. Gómez, L. Fabbrizzi, M. Licchelli, E. Monzani, *J. Am. Chem. Soc.* **2004**, *126*, 16507.
13 S. Yamaguchi, S. Akiyama, K. Tamao, *J. Am. Chem. Soc.* **2001**, *123*, 11372.
14 T. Gunnlaugsson, A. P. Davis, M. Glynn, *Chem. Commun.* **2001**, 2556.
15 T. Gunnlaugsson, A. P. Davis, J. E. O'Brien, M. Glynn, *Org. Lett.* **2002**, *4*, 2449.
16 R. Miao, Q.-Y. Zheng, C.-F. Chen, Z.-T. Huang, *Tetrahedron Lett.* **2005**, *46*, 2155.
17 S. K. Kim, N. J. Singh, S. J. Kim, K. M. K. Swamy, S. H. Kim, K.-H. Lee, K. S. Kim, J. Yoon, *Tetrahedron* **2005**, *61*, 4545.
18 Y. Kubo, M. Tsukahara, S. Ishihara, S. Tokita, *Chem. Commun.* **2000**, 653.
19 S. K. Kim, J. Yoon, *Chem. Commun.* **2002**, 770.
20 S. Nishizawa, H. Kaneda, T. Uchida, N. Teramae, *J. Chem. Soc., Perkin Trans. 2* **1998**, 2325.
21 K. Choi, A. D. Hamilton, *Angew. Chem., Int. Ed.* **2001**, *40*, 3912.
22 E. J. Cho, J. W. Moon, S. W. Ko, J. Y. Lee, S. K. Kim, J. Yoon, K. C. Nam, *J. Am. Chem. Soc.* **2003**, *125*, 12376.
23 C. B. Black, B. Andrioletti, A. C. Try, C. Ruiperez, J. L. Sessler, *J. Am. Chem. Soc.* **1999**, *121*, 10438.
24 H. Miyaji, P. Anzenbacher, Jr., J. L. Sessler, E. R. Bleasdale, P. A. Gale, *Chem. Commun.* **1999**, 1723.
25 P. Anzenbacher, Jr., K. Jursikova, J. L. Sessler, *J. Am. Chem. Soc.* **2000**, *122*, 9350.
26 C.-H. Lee, H.-K. Na, D.-W. Yoon, D.-H. Won, W.-S. Cho, V. M. Lynch, S. V. Shevchuk, J. L. Sessler, *J. Am. Chem. Soc.* **2003**, *125*, 7301.
27 G. A. Jeffrey, *An Introduction to Hydrogen Bonding*, Oxford University Press, New York, **1997**.
28 S. Fery-Forgues, M. T. Le Bris, J. Guette, B. Valeur, *J. Phys. Chem.* **1988**, *92*, 6233.
29 M. Kasha, *J. Chem. Soc., Faraday Trans. 2* **1986**, *82*, 2379.
30 Y. Nishimura, M. Kamada, M. Ikegami, R. Nagahata, T. Arai, *J. Photochem. Photobiol., A* **2006**, *178*, 150.
31 N. Boens, N. Tamai, I. Yamazaki, T. Yamazaki, *Photochem. Photobiol.* **1990**, *52*, 911.